JVI Journals.ASM.org

Mitogen-Activated Protein Kinase-Interacting Kinase Regulates mTOR/AKT Signaling and Controls the Serine/Arginine-Rich Protein Kinase-Responsive Type 1 Internal Ribosome Entry Site-Mediated Translation and Viral Oncolysis

Michael C. Brown,[a,b] Mikhail I. Dobrikov,[b] Matthias Gromeier[a,b]

Department of Molecular Genetics and Microbiology[a] and Department of Surgery, Division of Neurosurgery, Duke University Medical Center, Durham, North Carolina, USA[b]

ABSTRACT

Translation machinery is a major recipient of the principal mitogenic signaling networks involving Raf-ERK1/2 and phosphoinositol 3-kinase (PI3K)-mechanistic target of rapamycin (mTOR). Picornavirus internal ribosomal entry site (IRES)-mediated translation and cytopathogenic effects are susceptible to the status of such signaling cascades in host cells. We determined that tumor-specific cytotoxicity of the poliovirus/rhinovirus chimera PVSRIPO is facilitated by Raf-ERK1/2 signals to the mitogen-activated protein kinase (MAPK)-interacting kinase (MNK) and its effects on the partitioning/activity of the Ser/Arg (SR)-rich protein kinase (SRPK) (M. C. Brown, J. D. Bryant, E. Y. Dobrikova, M. Shveygert, S. S. Bradrick, V. Chandramohan, D. D. Bigner, and M, Gromeier, J. Virol. 22:13135–13148, 2014, doi:http://dx.doi.org/10.1128/JVI.01883-14). Here, we show that MNK regulates SRPK via mTOR and AKT. Our investigations revealed a MNK-controlled mechanism acting on mTORC2-AKT. The resulting suppression of AKT signaling attenuates SRPK activity to enhance picornavirus type 1 IRES translation and favor PVSRIPO tumor cell toxicity and killing.

IMPORTANCE

Oncolytic immunotherapy with PVSRIPO, the type 1 live-attenuated poliovirus (PV) (Sabin) vaccine containing a human rhinovirus type 2 (HRV2) IRES, is demonstrating early promise in clinical trials with intratumoral infusion in recurrent glioblastoma (GBM). Our investigations demonstrate that the core mechanistic principle of PVSRIPO, tumor-selective translation and cytotoxicity, relies on constitutive ERK1/2-MNK signals that counteract the deleterious effects of runaway AKT-SRPK activity in malignancy.

Translation of picornaviral RNAs occurs via cap-independent recruitment of preinitiation complexes (PICs) (comprising 40S subunits, eukaryotic initiation factor (eIF) 2-GTP-tRNA$_i^{Met}$ ternary complexes, eIF3, and eIF1/1A) by type 1 (e.g., enterovirus [1]) or type 2 (e.g., cardiovirus and aphthovirus [2]) internal ribosomal entry sites (IRESs). Two (vertebrate host) virus IRES mechanisms with distinct translation factor involvement have been delineated: (i) direct, eIF4F-independent PIC engagement (e.g., at the hepatitis C virus [HCV] IRES [3]) and (ii) recruitment of PICs via the eIF4G/4A/4B translation initiation helicase complex to type 1 (4) or type 2 (5) IRESs. The eIF4G/4A/4B complex, a dynamic aggregate of three RNA-binding proteins (6), can associate with viral (or select eukaryotic) RNAs independently of a 5′ terminus, a 5′-terminal 7-methyl-guanidine (m^{7}G) cap, or the cap-binding protein, eIF4E. Contact with IRESs is established by the "core" region of eIF4G (in eIF4G1, approximately amino acids [aa] 712 to 970), the Huntington/elongation factor 3/protein phosphatase 2A/TOR (HEAT) domain 1, which interacts with eIF4A/4B and RNA (7, 8). Noncanonical PIC tethering that lacks stabile recruitment of eIF4F (at the m^{7}G cap) may explain the involvement of RNA-binding proteins (IRES *trans*-acting factors [ITAFs]) in picornaviral type 1 IRES-mediated translation. While a number of RNA-binding proteins have been shown to associate with type 1 IRESs in various contexts/assays, the strongest empirical support for ITAF activity exists for the poly(rC)-binding protein 2 (PCBP2) (9). This is because recent evidence directly implicates PCBP2 in PIC recruitment *in vitro* (4). The precise mechanism of PCBP2's involvement remains unclear but requires the SR protein SRp20 (10).

All key factors involved in PIC recruitment to picornaviral type 1 IRESs are subject to regulatory adjustment through mitogenic signal transduction networks. This explains why viral IRES competence is influenced by the prevailing signaling status in host cells. PVSRIPO, the live-attenuated poliovirus (PV) (Sabin) type 1 vaccine replicating under the control of a foreign human rhinovirus type 2 (HRV2) IRES, is profoundly neuron incompetent due to cell-type-specific deficits in PIC recruitment to its heterologous IRES (11). However, PVSRIPO translation, cytotoxicity, and cell killing are retained in malignant cells, e.g., those derived from glioblastoma (GBM) (12). We report in an accompanying study that type 1 IRES efficiency generally, and tumor competence of PVSRIPO specifically, is facilitated by Raf-ERK1/2 signals and the

Received 28 June 2014 **Accepted** 26 August 2014
Published ahead of print 3 September 2014
Editor: D. S. Lyles
Address correspondence to Matthias Gromeier, grome001@mc.duke.edu.

doi:10.1128/JVI.01884-14

ERK1/2 substrate mitogen-activated protein kinase (MAPK)-interacting kinase (MNK) in particular (13).

Our studies implicate MNK in IRES competence independently of its classic functions as an eIF4G binding partner (14, 15) or eIF4E(S209) kinase (16). Rather, viral translation responded to MNK-mediated effects on the Ser/Arg (SR)-rich protein kinases 1 and 2 (SRPK1/2), which regulate splicing, mRNA export, and translation by phosphorylating the SR proteins (13). An important question raised by our investigations is the mechanism by which MNK controls SRPK (and its downstream substrates). Here, we show that MNK1 activity modulates SRPK through negative regulation of mTORC2 and its substrate, AKT. Our results are consistent with recent reports ascribing a predominant role to AKT signals in control of SRPK partitioning and activity in posttranscriptional gene regulation (17). In line with our findings, direct inhibition of mTORC2-mediated phosphorylation of AKT stimulated PVSRIPO translation and prevented the repression of PVSRIPO translation caused by MNK inhibition. Moreover, we present evidence suggesting that the inhibition of mTORC2-AKT by MNK may be a consequence of (MNK-mediated) stimulation of mTORC1. Thus, PVSRIPO translation competence is responsive to a signaling network centered on MNK that counters AKT phosphorylation and activity by regulating mTOR signaling.

MATERIALS AND METHODS

Cell lines, viruses, stimulants, inhibitors, and infections. Wild-type (wt) and MNK1/2 double-knockout (dko) mouse embryo fibroblasts (MEFs) (18) and Du54, 43, U87, and HeLa R19 cells were grown in Dulbecco's modified Eagle's medium (DMEM) containing 10% fetal bovine serum (FBS). Stable doxycycline (Dox)-inducible HeLa cell lines (19) were grown in DMEM supplemented with 10% FBS, 2.5 μg/ml blasticidin S (Sigma-Aldrich), and 100 μg/ml hygromycin B (Invitrogen). Dox-inducible MNK(D191A) and MNK(T334D) cell lines have been described previously (13). PVSRIPO was described previously (20) and propagated as described previously (13). 12-*O*-Tetradecanoylphorbol-13-acetate (TPA) (Tocris) or insulin-like growth factor 1 (IGF1) (Sigma) were dissolved in dimethyl sulfoxide (DMSO) and sterile water, respectively. Inhibitors of phosphoinositol 3-kinase (PI3K) (PI103; Tocris), mTORC1 (rapamycin [rapa]; Sigma), mTORC1/C2 (torin2; Tocris), MNK (CGP57380; Tocris), and SRPK (SRPin340; Millipore) were dissolved in DMSO and used as described in the figure legends. Dox (Sigma) was dissolved in sterile water and used at a concentration of 1 μg/ml. All infections were carried out at a multiplicity of infection (MOI) of 5, as previously described (13). ATP release assays were performed as reported previously (13).

siRNA, Mnk expression assays, and RNA reporters. For small interfering RNA (siRNA) transfections, 1×10^5 cells were seeded in 35-mm dishes (MNK depletion) or 2×10^4 cells/well were seeded in a 24-well plate (all other depletions) and transfected the following day. All-Stars nontargeting control (Ctrl) siRNA or siRNA targeting MNK1, SRPK1/2, raptor, or rictor (Qiagen) were transfected (50 pmol/35-mm dish or 12.5 pmol/well for a 24-well plate) using Lipofectamine 2000 (Invitrogen) following the manufacturer's protocol. The cells were used 60 to 72 h posttransfection for further experiments. For MNK overexpression assays, Dox was added at the time points (hours prior to harvest) indicated in the figures. HRV2, coxsackievirus B3 (CBV3), HCV, and β-globin reporter plasmids (21) were used for *in vitro* transcription, transfection, and analysis, as described in reference 13, but scaled down to a 24-well-plate format. For reporter assays in IGF1/siSRPK-treated cells, the IRES (*Renilla* luciferase [rluc]) versus m^7G cap (firefly luciferase [fluc]) ratios were determined. Assays were normalized by dividing plus-IGF1/siSRPK and plus-IGF1/siCtrl ratios by minus-IGF1/siCtrl ratios.

Antibodies, immunoblotting, and immunofluorescence staining. Cell lysates were prepared using polysome lysis buffer, and immunoblots were performed as previously described (22). The antibodies used in this study were specific to PV 2C/2BC (23), phosphorylated AKT(S473) [p-AKT(S473)], p-AKT(T308), AKT, p-ERK1/2, ERK1/2, p-S6K(T389), S6K, ribosomal protein S6 (rpS6), p-rpS6(SS240/4), MNK1, p-eIF4E(S209), eIF4E, hemagglutinin (HA), raptor, and rictor (all from Cell Signaling); tubulin (Sigma-Aldrich); and SF2 (Novus). For raptor/rictor depletion assays, the immunoblots for viral protein 2C (see Fig. 8C) were analyzed in a manner to permit comparison of viral IRES competency in cells with uneven baseline viral propagation (due to viability effects of the raptor/rictor depletions). The filters were subjected to 10 different exposures from a representative experiment, and the DMSO vehicle control values were measured by densitometry using image J (http://imagej.nih.gov/ij/). Exposures with equal control 2C levels were used for each siRNA. As for all other immunoblots, the quantitated bar graph data (see Fig. 8C) were obtained using a Licor Odyssey with all samples on the same blot for each independent experiment. For indirect immunofluorescence (IF) staining, cells were grown on coverslips and fixed using methanol at −20°C (15 min). Staining for SF2 was performed as described in the accompanying article (13), and the slides were photographed using an Olympus IX71 fluorescence microscope.

Statistics. Quantitated immunoblot/reporter values were represented as averages and standard errors of the mean (SEM) and were normalized between independent experiments as described in the figure legends. Paired Student *t* tests (used only to compare two groups) or analysis of variance (ANOVA)-protected *t* tests (allowing multiple comparisons within a data group) were performed using JMP10 (SAS). Significance was defined as a P value of <0.05, and the tests used for each data group are described in the figure legends.

RESULTS

Our previous observations indicated that PVSRIPO translation, cytotoxicity, and killing of GBM (i) are stimulated by MNK1/2 catalytic activity; (ii) are blocked by MNK1 depletion/MNK inhibition; and (iii) are enhanced by eIF4G-independent, MNK-mediated effects on SRPK (13). MNK inhibition/depletion was associated with events consistent with SRPK nuclear influx and nuclear-speckle dissociation. MNK effects on PVSRIPO translation and cancer cytotoxicity depend on SRPK, because repression of viral translation/cytotoxicity by MNK depletion or inhibition was reversed by concomitant SRPK depletion/inhibition (13). SRPK depletion alone, in the absence of MNK activation, strongly enhanced PVSRIPO translation and propagation (13). Our investigations raise important questions about the mechanism of MNK-mediated effects on SRPK (and its downstream effectors, the SR proteins). MNK may affect SRPK directly, e.g., through posttranslational changes to its immediate regulatory context, or it may act indirectly, through a broader signal transduction network known to control SRPK subcellular partitioning and activity.

MNK inhibition and AKT activation have similar effects on SRPK. Prior investigations of SRPK and alternative splicing control via activation of the epidermal growth factor receptor tyrosine kinase, which signals to Raf-ERK1/2-MNK and PI3K-AKT, suggested a critical role for the PI3K-AKT signaling axis (17). AKT, which was shown to bind SRPK1, induces its autophosphorylation, dissociates it from its cytoplasmic "anchor," and promotes SRPK1 activity through nuclear influx (17). To avoid confounding effects of dual activation of Raf-ERK1/2-MNK and PI3K-AKT in our assays, we used selective induction of PI3K-AKT signaling with IGF1 (the signaling scheme is shown in Fig. 1). IGF1 treatment of cells induced strong PI3K-AKT activation, without concomitant effects on ERK1/2 (for at least 4 to 5 h) (Fig. 2A and B).

In accordance with the findings of Zhou et al. (17), selective

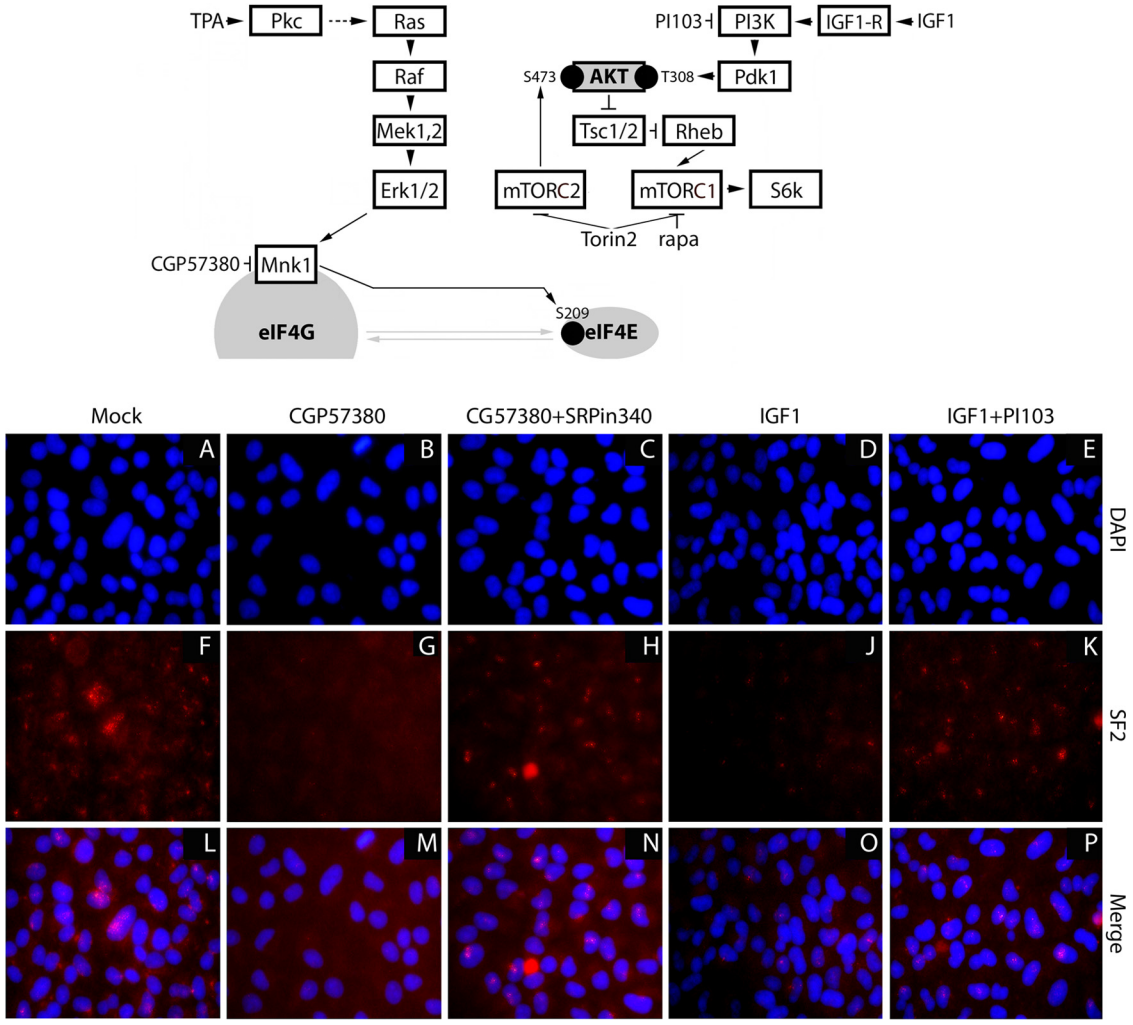

FIG 1 Activation of PI3K-AKT has effects on SRPK similar to those of MNK inhibition. (Top) Signaling scheme and inhibitors used. (Bottom) IF of the nuclear-speckle marker and SRPK substrate SF2 in HeLa cells treated with DMSO (A, F, and L), CGP57380 (10 μM) (B, G, and M), CGP57380 plus SRPin340 (10 μM and 3 μM, respectively) (C, H, and N), IGF1 (10 nM) (D, J, and O), and IGF1 plus PI103 (10 nM and 1 μM, respectively) (E, K, and P) for 2 h.

activation of PI3K-AKT led to nuclear-speckle dissociation (Fig. 1J and O), indicating SRPK activation. The IGF1 effect was prevented by PI3K inhibition, implicating PI3K-AKT in this event (Fig. 1K and P). MNK's influence on SRPK partitioning, evident as nuclear-speckle dissociation upon MNK1 depletion (13), is equally manifest with MNK inhibition with CGP57380 (Fig. 1G and M). CGP57380-mediated speckle dissociation is due to MNK-mediated effects on SRPK, because adding the SRPK inhibitor SRPin340 reverses the effect of CGP57380 (Fig. 1H and N). Thus, activation of PI3K-AKT (with IGF1) and MNK1 depletion (13) or inhibition have similar effects on SRPK partitioning and activity.

Activation of AKT represses IRES competence. Our observations emerging from these tests and our prior findings (13) suggest opposing effects on SRPK and its role in IRES-mediated translation competence: repression through activation of Raf-ERK1/2-MNK and activation through PI3K-AKT. If this is true, then outright activation of AKT may have opposite (repressive) effects on IRES competence compared to activation of MNK. To test this, we selectively activated PI3K-AKT signaling by treating cells with IGF1 (10 nM) and assessing the effect on PVSRIPO/HRV2 IRES-mediated translation (Fig. 2A). Within the testing interval of the assay, IGF1 led to strong phosphorylation of AKT(S473/T308) without changing the ERK1/2 phosphorylation status (Fig. 2A). This was associated with an ~60% decrease of viral translation at 4.5 h postinfection (p.i.) (Fig. 2A). The effect was overcompensated for by PI3K inhibition (with PI103) (Fig. 2A), but not by mTORC1 inhibition with rapa, suggesting that it involves signaling upstream of mTORC1 or a rapa-insensitive function of mTORC1 (Fig. 2B). Inhibition of SRPK with SRPin340 abolished the repressive effect of IGF1 on viral translation, suggesting that PI3K-AKT activation acts on IRES competence via SRPK (Fig. 2B). These data further implicate SRPK in PVSRIPO translation competence/tumor cytotoxicity. They illustrate how activating (via PI3K-AKT) or repressing (via ERK1/2-MNK) SRPK exerts opposing effects on IRES competence, possibly through a common mechanism.

To irrevocably link the observed signaling events to IRES-mediated translation of viral genomes, we tested the effect of AKT activation and concomitant SRPK inhibition on IRES-reporter translation in HeLa cells (Fig. 2C) and on PVSRIPO cytotoxicity

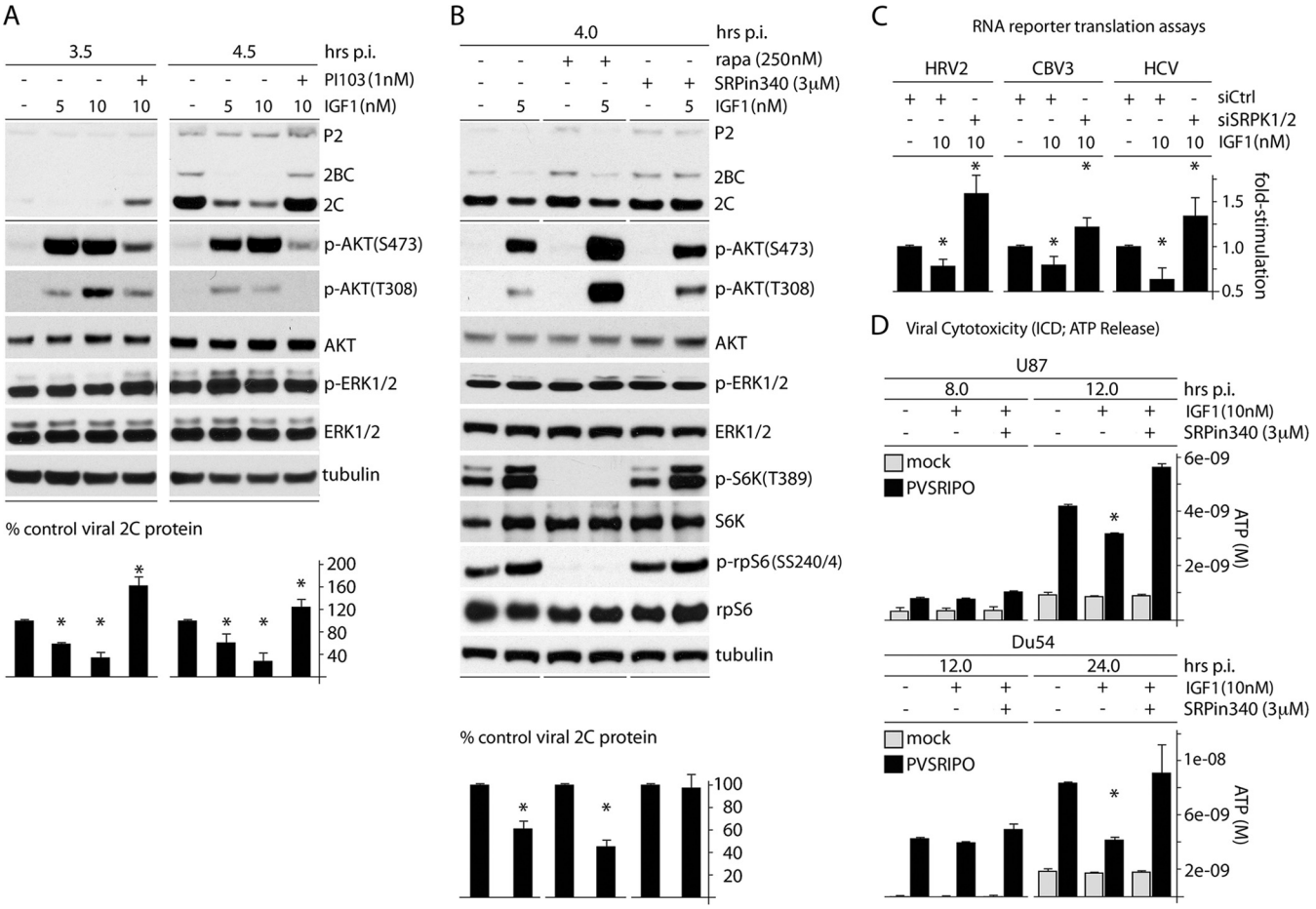

FIG 2 AKT signals negatively affect PVSRIPO translation and cytotoxicity through SRPK. (A) Cells were treated with IGF1 (5 or 10 nM) and PI103 (1 nM) as shown 1 h prior to infection and throughout the assay. Cells were harvested at 3.5 and 4.5 h p.i. and analyzed by immunoblotting. Viral protein 2C was quantitated for 3 experiments and normalized by setting the IGF1 (−) control to 100%. (B) Cells were pretreated with IGF1 (5 nM) or mock pretreated in the presence of DMSO, rapa (250 nM), or SRPin340 (3 μM) 1 h before infection and throughout the assay. Quantitation of viral protein 2C was determined from 3 assays and normalized by setting the IGF1 (−) control for each condition to 100%. The asterisks indicate Student's *t* test comparing IGF-treated lanes to DMSO-treated controls for each pretreatment ($P < 0.05$). (C) Cells were treated with siCtrl or siSRPK1/2 (72 h), pretreated with IGF1 (10 nM; 1 h), and then cotransfected with fluc and rluc reporters. IGF1 stimulation was maintained after transfection, and cells were harvested at 4 h for fluc/rluc measurements. The assay was performed in duplicate for 3 tests, and the average fold stimulation values were determined and normalized by setting siCtrl (without IGF1) to 1. (D) Glioma cells were mock treated or treated with IGF1 in the presence of DMSO or SRPin340 (3 μM) and mock infected or infected with virus, and the supernatants were collected at the designated intervals and tested for ATP release. (A, C, and D) The asterisks represent ANOVA-protected *t* tests ($P < 0.05$). The error bars indicate SEM.

and cell killing in GBM cells (Fig. 2D). In accordance with our findings on PVSRIPO translation upon IGF1 stimulation (Fig. 2A and B), translation of IRES-reporter RNAs (HRV2, CBV3, and HCV) was depressed upon treatment of cells with IGF1 (Fig. 2C). This effect was reversed by concomitant depletion of SRPK1/2 (Fig. 2C). Indeed, SRPK depletion (in the presence of IGF1) produced IRES-reporter translation rates in excess of baseline, indicating a role for SRPK in control of basal viral cap-independent translation (Fig. 2C). Similar effects of IGF1 and IGF1 plus SRPK inhibition was observed with PVSRIPO cytotoxicity in GBM cells (Fig. 2D). These findings and the observation that MNK inhibition effects on PVSRIPO translation are due—at least in part—to SRPK activation (13) indicate that ERK1/2-MNK and PI3K/AKT signals regulate PVSRIPO translation through a common effector, SRPK.

MNK acts on SRPK via AKT. Our findings may be the result of separate, opposing effects of active MNK and AKT on the SRPK system, or they could suggest that MNK acts on SRPK by tempering AKT activity (consistent with reports linking AKT directly to SRPK1 [17]). To test these possibilities, we analyzed the effects of TPA stimulation/MNK1 depletion on AKT activity (Fig. 3). Phosphorylation of both AKT(S473) by mTORC2 and AKT(T308) by PDK1 (24) (Fig. 1, top) is required for full activation of the kinase. TPA stimulation of cells depressed p-AKT(S473) by ~40% (Fig. 3A). However, in TPA-stimulated cells depleted of MNK1, p-AKT levels were elevated ~4-fold compared to nondepleted cells (Fig. 3A). To confirm these results without the potential off-target effects of signal inducers or inhibitors or siRNAs, we used a Dox-inducible MNK1 overexpression assay (13). This permitted us to evaluate the effects of selective MNK activation achieved with Dox induction alone. Expression of constitutively active MNK1(T334D) consistently depressed p-AKT (S473) levels to below 40%, while expression of kinase-dead MNK1(D191A) had no effect (Fig. 3B). Also, MNK inhibition

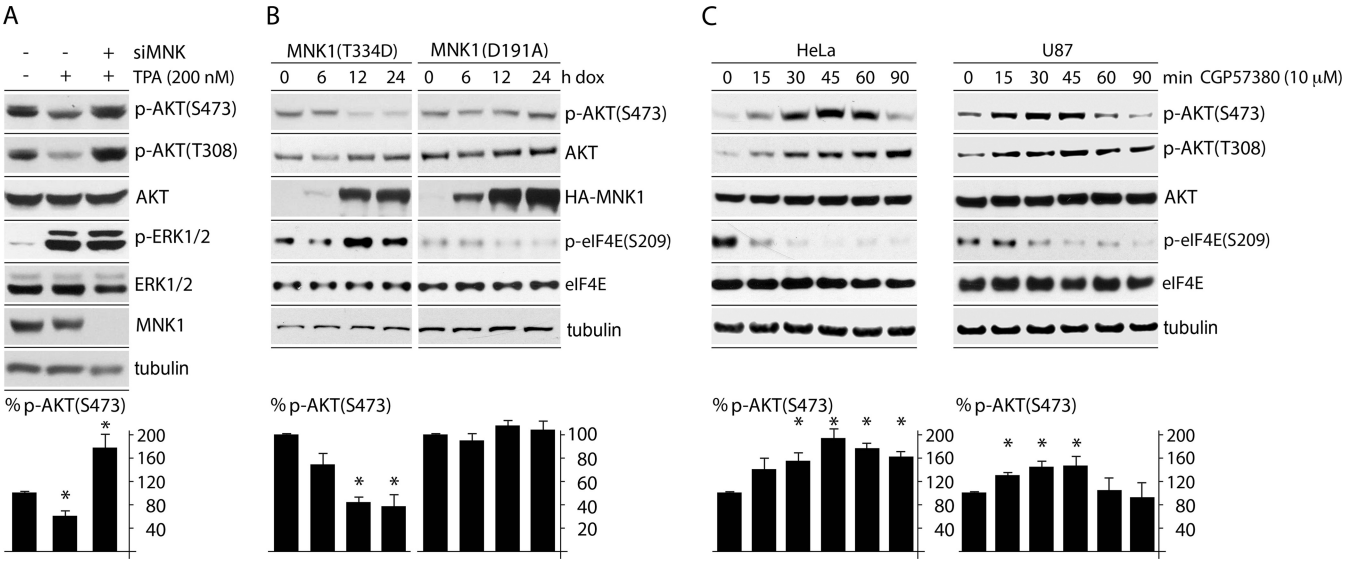

FIG 3 MNK1 activation leads to depression of AKT phosphorylation. (A) HeLa cells treated with siCtrl (with or without TPA) or siMNK (plus TPA) were lysed and tested by immunoblotting for p-AKT(S473/T308), and the percent phosphorylation was calculated from the average of 3 tests, setting siCtrl (without TPA) to 100%. (B) Constitutively active MNK1(T334D) or kinase-dead MNK1(D191A) expression was Dox induced at the designated time points. p-AKT(S473) was quantitated from 3 independent assays, setting the 0-h (plus-Dox) time point to 100%. (C) HeLa and U87 glioma cells were treated with CGP57380 (10 μM) for the indicated intervals and analyzed by immunoblotting. p-AKT(S473) was quantitated and averaged between 3 experiments. Quantitation between experiments was normalized by setting the 0-min CGP57380 value to 100%. The error bars represent SEM, and the asterisks represent ANOVA-protected *t* tests ($P < 0.05$).

in HeLa and U87 GBM cells with CGP57380 increased p-AKT (S473) levels (Fig. 3C). At later time points (>60 min after CGP57380 treatment), p-AKT(S473) levels tapered off, suggesting that feedback may restore the equilibrium of the system after prolonged MNK inhibition (Fig. 3C).

For independent corroboration of these results in a different system (in cells with wild-type PTEN), we tested the response of MNK1/2 dko MEFs to IGF1 and to CGP57380. Serendipitously, we found that AKT levels were increased relative to tubulin and other loading controls in dko MEFs (compared to wt companion MEFs) (Fig. 4A). This may represent an increase in basal signaling to AKT, as AKT(T450) is cotranslationally phosphorylated by mTORC2 to stabilize nascent AKT protein (25). In the preceding assay, we stimulated wt or MNK1/2 dko MEFs with IGF1 (60 min) in the presence of DMSO (60 min) or CGP57380 (30 and 60 min) to compare (i) IGF1-mediated AKT activation in contexts with and without MNK and (ii) CGP57380-mediated p-AKT(S473/T308) modulation (Fig. 4B). First, we observed that the overall

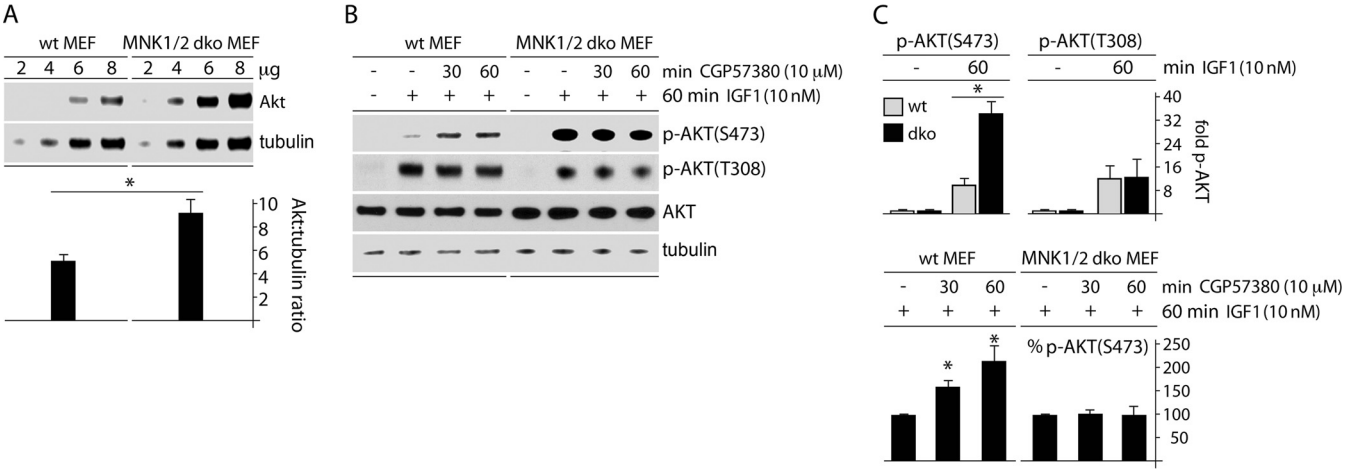

FIG 4 MNK1 activation leads to depression of AKT phosphorylation in mouse MEFs. (A) Wt or MNK1/2 dko MEF lysates were compared by immunoblotting for total AKT versus tubulin contents. Quantitation is shown below, representing the AKT/tubulin ratio to correct for loading anomalies; the asterisk represents Student's *t* test ($P < 0.05$). (B) Wt or dko MEFs were mock treated or IGF1 treated (60 min) in the presence of DMSO (60 min) or CGP57380 (10 μM; 30 or 60 min, as indicated) and analyzed for p-AKT(S473) and p-AKT(T308) by immunoblotting. (C) (Top) Quantitation of p-AKT(S473) and p-AKT(T308) in wt and dko MEFs after treatment with IGF1 (10 nM; 60 min). The values were normalized by setting samples without IGF1 to 1. (Bottom) Quantitation of p-AKT(S473) from the experiment in panel B. Values were normalized between experiments by setting IGF1 plus DMSO (B, lanes 2 and 6 from left) to 100%. The error bars represent SEM, the asterisks directly over bars represent ANOVA-protected *t* tests ($P < 0.05$), and the asterisks over lines represent Student *t* tests ($P < 0.05$).

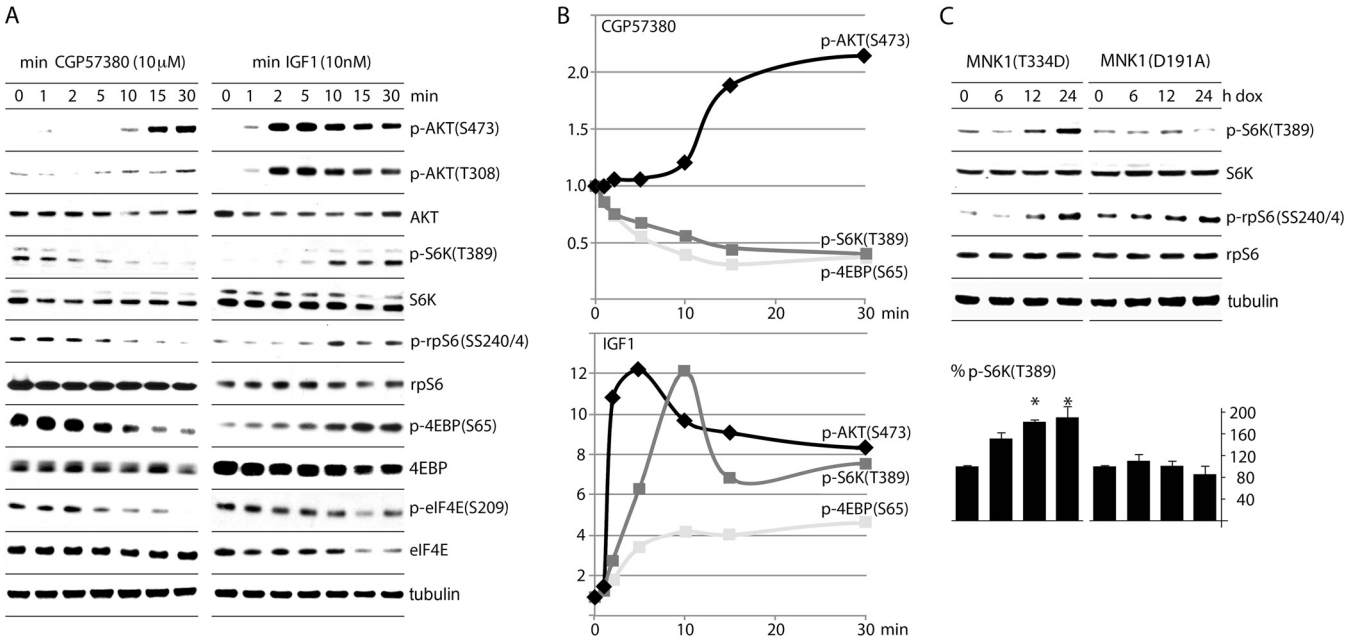

FIG 5 CGP57380 and IGF1 treatments induce AKT(S473) phosphorylation but have the opposite effect on substrates without mTORC1. (A) HeLa cells treated with 10 μM CGP57380 (left) or 10 nM IGF1 (right) were harvested at the designated time points for immunoblotting. (B) Quantitation of p-AKT(S473)/AKT, p-S6K(T389)/S6K, and p-4EBP(S65)/4EBP ratios for CGP57380 (top) and IGF1 (bottom). (C) Lysates from cells expressing Dox-inducible MNK1(T334D) or MNK1(D191A) (Fig. 3B) were tested for phosphorylation of S6K(T389); the averages of 3 independent assays with SEM are represented for p-S6K(T389), corrected by dividing by total S6K values. The asterisks denote ANOVA-protected *t* tests ($P < 0.05$) comparing Dox induction to a no-Dox control.

responsiveness of p-AKT(S473), but not p-AKT(T308), to IGF1 in MNK1/2 dko MEFs was significantly increased compared to wt MEFs (Fig. 4C, top). Furthermore, CGP57380, in the presence of IGF1, incrementally increased p-AKT(S473) levels in wt MEFs, but not in MNK1/2 dko MEFs (Fig. 4B and C, bottom). These observations suggest that MNK1 counters phosphorylation of AKT(S473), either by interfering with its upstream kinase (mTORC2) or through AKT-specific effects.

MNK inhibition enhances p-AKT(S473) and diminishes mTORC1 activity. In order to unravel the effects of MNK on AKT activity, we studied several relevant phosphorylation events in a time course comparing MNK inhibition with CGP57380 and AKT stimulation with IGF1 (Fig. 5). As expected, both CGP57380 and IGF1 led to a significant increase in p-AKT(S473) (Fig. 5A and B). p-AKT(T308) responded weakly to MNK inhibition, while IGF1 led to strong, sustained AKT(T308) phosphorylation (Fig. 5A). Intriguingly, IGF1 spurred p-AKT(S473) after 1 min, whereas CGP57380 did so only at 10 min (Fig. 5B). These data, combined with the observation that expression of constitutively active MNK1(T334D) suppressed p-AKT(S473) (Fig. 3B), suggest that MNK catalytic activity blocks phosphorylation of AKT(S473). Analysis of the phosphorylation status of the mTORC1 targets S6K (and its downstream substrate, rpS6) and the eIF4E-binding proteins (4EBPs) revealed that, while IGF1 enhanced mTORC1 activity ~8-fold by 10 min (p-S6K) (Fig. 5B), CGP57380 diminished mTORC1 activity >2-fold by 15 min (Fig. 5B). mTORC1 repression by CGP57380 occurred prior to the increase in p-AKT(S473) and coincided with the decline in p-eIF4E(S209), consistent with a primary effect of MNK.

It is possible that CGP57380 modulates mTORC1 or mTORC2 activity through effects on kinases other than MNK. Thus, to confirm an apparent role for MNK in stimulating mTORC1 in a different system devoid of inhibitors or stimulants, we used lysates from cells with Dox-induced, constitutively active (T334D) or kinase-dead (D191A) MNK1 to assess the phosphorylation status of mTORC1 targets (Fig. 5C) (the lysates used were those analyzed in Fig. 3B). Constitutively active MNK1(T334D) significantly enhanced p-S6K(T389) and p-rpS6(SS240/4), while kinase-dead MNK1 had no effect (Fig. 5C). This confirms a role for MNK catalytic activity in stimulating mTORC1 (Fig. 5C) while simultaneously inhibiting mTORC2 (Fig. 3B). Thus, MNK either favors mTORC1 formation/activation to inhibit mTORC2 [and thus, AKT(S473) phosphorylation] or MNK may influence AKT(S473) phosphorylation independently of its apparent role in regulating mTOR signaling.

MNK controls phosphorylation of AKT(S473) through modulation of mTORC2 activity. mTORC2 is believed to be a dominant kinase for AKT(S473) in most signaling contexts (24); however, other kinases were shown to be involved, e.g., integrin-linked kinase (26). To test if MNK regulates p-AKT(S473) through effects on mTORC2, we studied a short time course of CGP57380 inhibition/IGF1 stimulation in the presence of DMSO (vehicle control), rapa (selective mTORC1 inhibition), or torin2 (mTORC1/C2 coinhibition) (Fig. 1, top, and 6). Confirming the data in Fig. 3 and 5, both CGP57380 and IGF1 induced AKT(S473) phosphorylation in the presence of DMSO (Fig. 6A and B). Rapa treatment prior to CGP57380/IGF1 permitted similar effects on p-AKT(S473), suggesting that MNK-mediated effects on AKT occur independently of rapa-sensitive functions of mTORC1. However, torin2 dramatically reduced p-AKT(S473) basal levels and prevented its stimulation by CGP57380/IGF1 (Fig. 6A and B). This indicates that MNK inhibition of AKT(S473) phosphorylation depends on either mTORC2 or a

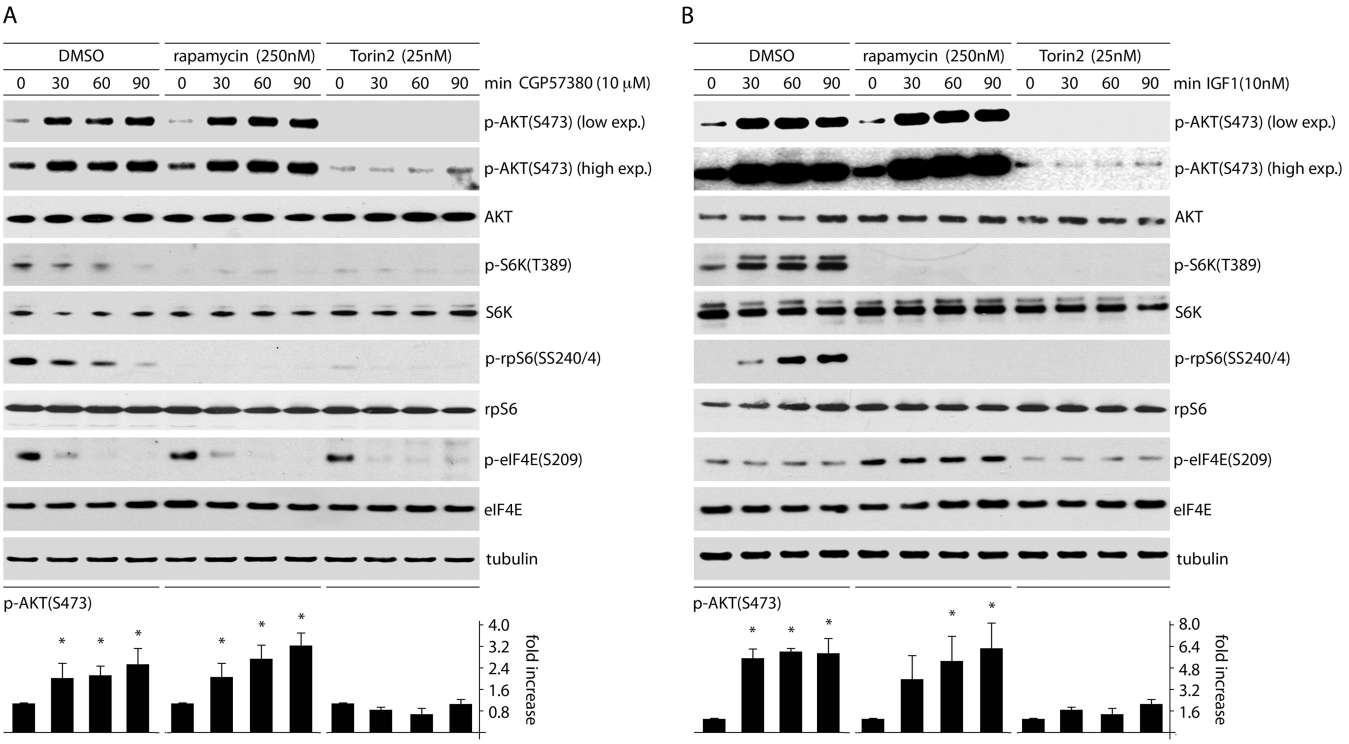

FIG 6 CGP57380- and IGF1-mediated effects on p-AKT(S473) occur through mTORC2. HeLa cells were pretreated with DMSO, rapa (250 nM), or torin2 (25 nM) (2 h). CGP57380 (10 μM) (A) or IGF1 (10 nM) (B) was added 0, 30, 60, or 90 min prior to cell lysis and analysis by immunoblotting. p-AKT(S473) was quantitated for 3 experiments for each time point, and the fold increase was determined by setting the zero time point for each group to 1. The error bars represent SEM, and the asterisks represent ANOVA-protected *t* tests comparing samples treated with CGP57380 or IGF1 to untreated controls.

rapa-insensitive function of mTORC1 and that, in the context of our assays, p-AKT(S473) levels are determined exclusively by mTORC2.

MNK inhibition suppresses type 1 IRES activity through a rapa-insensitive, mTOR-dependent mechanism. Since MNK counters mTORC2-mediated phosphorylation of AKT(S473) (and thus suppresses AKT activity) and inhibition of the AKT-SRPK axis (e.g., with PI3K inhibitors) stimulates PVSRIPO translation and cytotoxicity, torin2 should mimic the stimulatory effect of MNK catalytic activity on PVSRIPO. Indeed, torin2 treatment enhanced PVSRIPO translation ~4-fold and significantly increased viral propagation in HeLa cells (Fig. 7A). We next asked whether MNK-induced effects on p-AKT(S473) explain the effects of MNK inhibition/depletion on PVSRIPO translation and cytotoxicity. To investigate this, cells were pretreated with DMSO, rapa, or torin2 (2 h), followed by DMSO or CGP57380 treatment and PVSRIPO infection (Fig. 7B). The CGP57380-induced increase of p-AKT(S473) is subtle in this assay, because the study interval was 4 h after addition of the drug (Fig. 7B; the time course is shown in Fig. 3C). Analysis of viral 2C expression revealed that MNK inhibition decreased viral translation ~4-fold (Fig. 7B). The effects were similar in mock (DMSO)- and rapa-pretreated cells (Fig. 7B), suggesting that MNK inhibition does not act on viral IRES-mediated translation via a rapa-sensitive function of mTORC1. Pretreatment with torin2, however, significantly reduced the effect of MNK inhibition on viral translation (Fig. 7B). These observations suggest that the repressive effect of MNK inhibition on PVSRIPO translation is due to either regulation of mTORC2-AKT or a rapa-insensitve mTORC1 function. To confirm these relationships in a relevant context, we evaluated the effect of mTORC1/C2 inhibition (with torin2) on PVSRIPO translation and cell killing in GBM cell lines (Fig. 7C). Treatment with torin2 significantly enhanced PVSRIPO translation competence and GBM cytotoxicity (Fig. 7C). These data imply that MNK-mediated stimulation of PVSRIPO translation, propagation, and cytotoxicity depends on an mTOR function not prevented by rapa.

MNK inhibition activates mTORC2 by attenuating mTORC1 activity. Our data with rapa and torin2 (Fig. 7), coupled with our observation that MNK activity exerts inverse effects on mTORC1 versus mTORC2 activity (Fig. 5), raise the possibility that MNK represses mTORC2-p-AKT(S473) by activating mTORC1. mTORC1-mediated suppression of mTORC2 has been reported to occur through several mechanisms, for example, via (mTORC1-driven) S6K activation and downstream phosphorylation of rictor (27). To test this possibility, we siRNA depleted cells of raptor or rictor (essential components of mTORC1 and mTORC2, respectively [see Fig. 9]); treated them with DMSO (mock), CGP57380 (10 μM), or IGF1 (10 nM); and measured p-AKT(S473) levels (Fig. 8). Two siRNAs, each targeting raptor or rictor, were independently used to account for possible off-target effects caused by any single siRNA. Two raptor siRNAs consistently had opposite effects on basal p-AKT(S473) levels; one increased (Fig. 8A, lanes 4 to 6) and the other reduced (Fig. 8A, lanes 7 to 9) basal AKT(S473) phosphorylation. We ascribe these differences to distinct depletion efficiencies of the two siRNAs, possibly analogous to what has been observed with mild versus intense rapa treat-

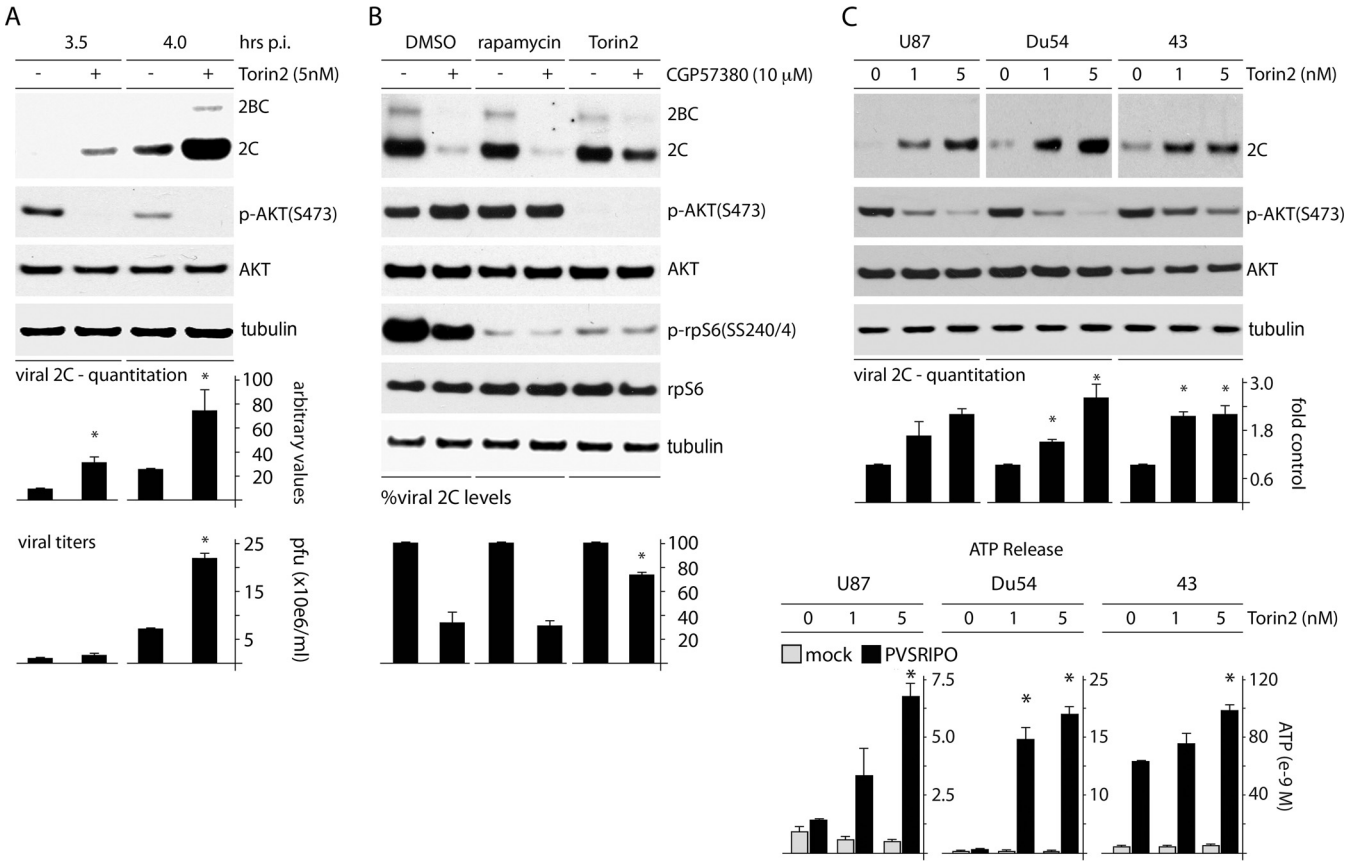

FIG 7 mTORC1/2 coinhibition synergizes with PVSRIPO oncolysis and prevents effects of MNK inhibition on PVSRIPO translation. (A) HeLa cells were infected with PVSRIPO and treated with either DMSO or torin2 (5 nM; 1 h p.i.). Cells were harvested (3.5 and 4 h p.i.) and analyzed for viral protein by immunoblotting. Quantitation from 3 assays is shown below; control values were normalized to one experiment for each time point. Viral titers were determined from supernatants of cells. The experiment was repeated twice, and control values were used to normalize between the assays. The error bars represent SEM; the asterisks denote Student's *t* test ($P < 0.05$). (B) HeLa cells were pretreated with DMSO, rapa (250 nM), or torin2 (25 nM) 1 h prior to treatment with DMSO or CGP57380 (10 μM) and infection with PVSRIPO. Inhibitors and DMSO were maintained during infection. Cells were harvested 3.5 h p.i. and analyzed by immunoblotting for viral protein and relevant controls. Quantitation is shown below from 3 assays normalized by setting control values (DMSO treated for each inhibitor group) to 100%. The statistics were done by comparing groups to the DMSO-plus-CGP57380-treated lane in an ANOVA-protected *t* test ($P < 0.05$). (C) (Top) GBM cells were infected and treated with DMSO (mock) or torin2 (1 or 5 nM) at the time of infection. Lysates were prepared 6 h p.i. and analyzed for viral protein by immunoblotting. Viral 2C protein was quantitated for 3 tests. (Bottom) GBM cells were infected with PVSRIPO and mock or torin2 (1 or 5 nM) treated 4 h p.i. The supernatants were collected 12 h p.i. and analyzed for ATP concentrations in 2 assays. The error bars represent SEM, and the asterisks indicate ANOVA-protected *t* tests ($P < 0.05$).

ment of cells (28) (Fig. 8A). Raptor depletion reduced basal S6K(T389) phosphorylation in line with residual raptor levels (Fig. 8A, compare lanes 1, 4, and 7), suggesting mTORC1 inhibition. It also diminished the inhibitory effect of CGP57380 on p-S6K(T389) (Fig. 8A, compare lanes 2 and 5). This is consistent with our finding that MNK inhibition (CGP57380) acts on p-S6K via mTORC1 (Fig. 5). S6K phosphorylation upon IGF1 stimulation was resistant to raptor depletion (Fig. 8A, lanes 3, 6, and 9), likely because of the potent stimulation it exerts on mTORC1 signaling and the incomplete raptor depletion. Intriguingly, CGP57380-mediated stimulation of AKT(S473) phosphorylation was reduced by both siRNAs (Fig. 8A). As anticipated, raptor depletion did not affect the AKT phosphorylation response to IGF1, since IGF1 activates AKT independently of mTORC1 (Fig. 8A). Depletion of rictor significantly reduced basal p-AKT(S473) and tempered the increase in p-AKT(S473) caused by both CGP57380 and IGF1 (Fig. 8B). This was expected, since mTORC2 is the kinase for AKT(S473) in most contexts (24). Taken together, our findings suggest that increased p-AKT(S473) in response to MNK inhibition requires both mTORC1 and mTORC2 activity and supports the hypothesis that MNK activates mTORC1, consequently diminishing mTORC2-mediated AKT(S473) phosphorylation.

Raptor and rictor depletion diminishes the effect of MNK inhibition on PVSRIPO translation. To test if MNK's effect on PVSRIPO is exerted through mTORC1-mediated mTORC2-AKT suppression, we evaluated viral translation in cells treated with siCtrl or one of two siRNAs targeting raptor or rictor (Fig. 8C). Raptor or rictor depletion mitigated the effect of MNK inhibition on PVSRIPO translation to various degrees, in accordance with the depletion efficiency (see Materials and Methods for test details) (Fig. 8C). These data suggest that MNK enhances PVSRIPO translation by acting on (rapa-resistant) mTORC1 to impede mTORC2-AKT activation. The resulting negative regulation of AKT reduces SRPK activation and enables PVSRIPO translation and cytotoxicity (a summary of the proposed mechanism is shown in Fig. 9).

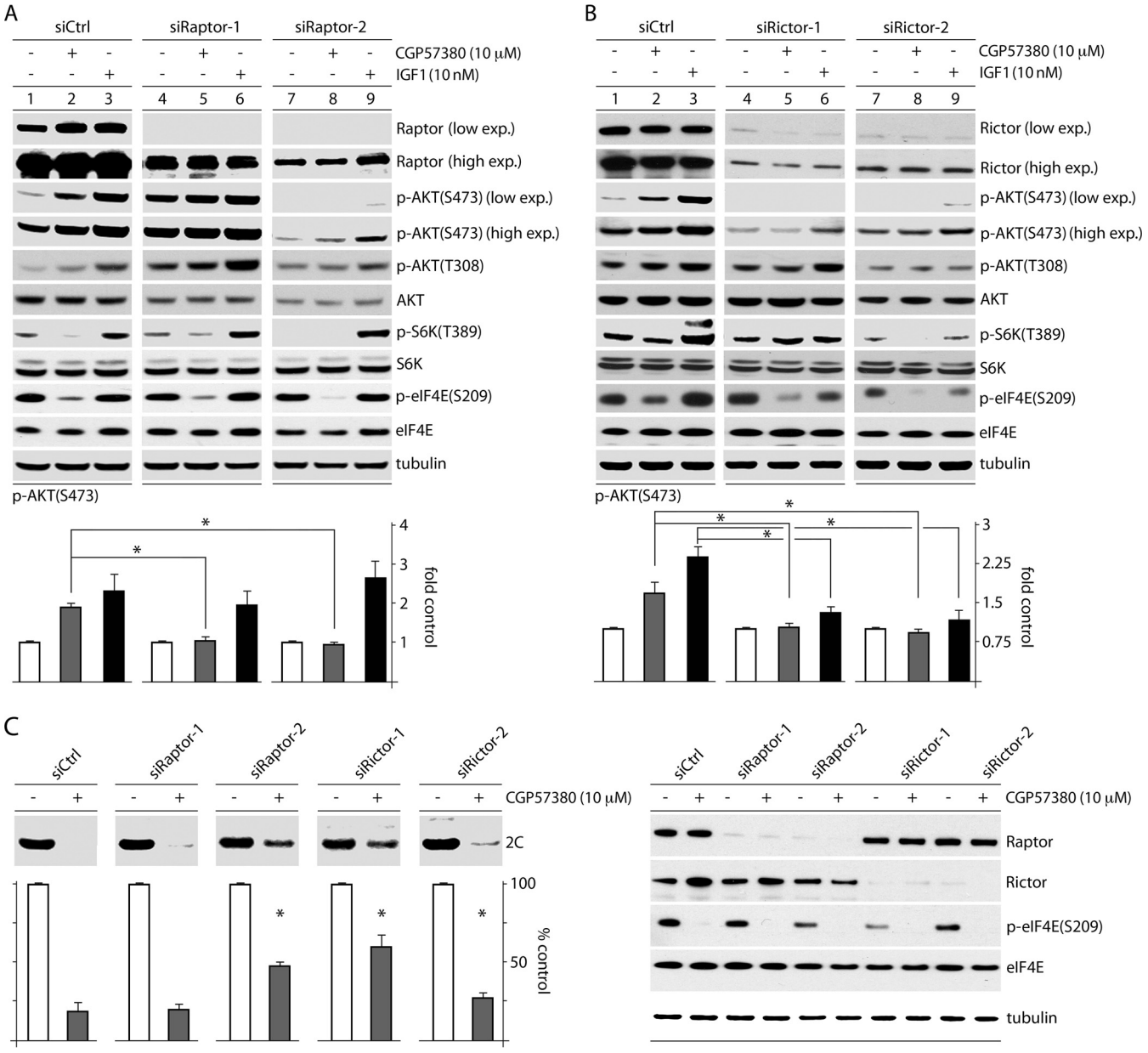

FIG 8 MNK inhibition affects AKT phosphorylation and PVSRIPO translation through mTORC1-mediated inhibition of mTORC2. HeLa cells were treated with siCtrl or one of two siRNAs targeting raptor (A) or rictor (B), followed by treatment with DMSO, CGP57380, or IGF1 (60 min). Cells were harvested and analyzed by immunoblotting for AKT phosphorylation. p-AKT(S473) levels were quantitated as shown for 4 tests each, normalizing between experiments by setting DMSO-treated samples to 1. The asterisks denote ANOVA-protected *t* tests ($P < 0.05$), and the error bars represent SEM. (C) HeLa cells were transfected with siCtrl or one of two different siRNAs targeting raptor or rictor as in panels A and B, treated with CGP57380 (30 min), infected with PVSRIPO, and harvested (3.5 h p.i.). The lysates were assessed for viral protein (2C), which is quantitated below for 4 assays, normalizing between experiments by setting the DMSO control for each siRNA to 1 (see Materials and Methods). The asterisks indicate significant ANOVA-protected *t* tests compared to the siCtrl-plus-CGP57380 values. The error bars represent SEM.

DISCUSSION

We deciphered a link between MNK and SRPK that broadly enhances cap-independent translation initiation via type 1 picornavirus IRESs and, by extension, favors PVSRIPO oncolysis of GBM (13). Unfettered PVSRIPO translation, cytotoxicity, and killing in most tumor cells, including those derived from GBM (12), suggests that type 1 IRES competence benefits from the particular posttranscriptional gene-regulatory conditions of the malignant state. Indeed, MNK activity has been intricately associated with oncogenesis (29, 30), which may involve eIF4E(S209) phosphorylation (31), but the mechanisms of its involvement remain obscure (30). In the present study, we unravel a novel intersection between ERK1/2-MNK and mTOR-AKT signal transduction pathways that controls the partitioning and activity of SRPK (Fig. 9). Ultimately, these signaling events explain how MNK facilitates type 1 IRES function and PVSRIPO oncolysis. They also delineate

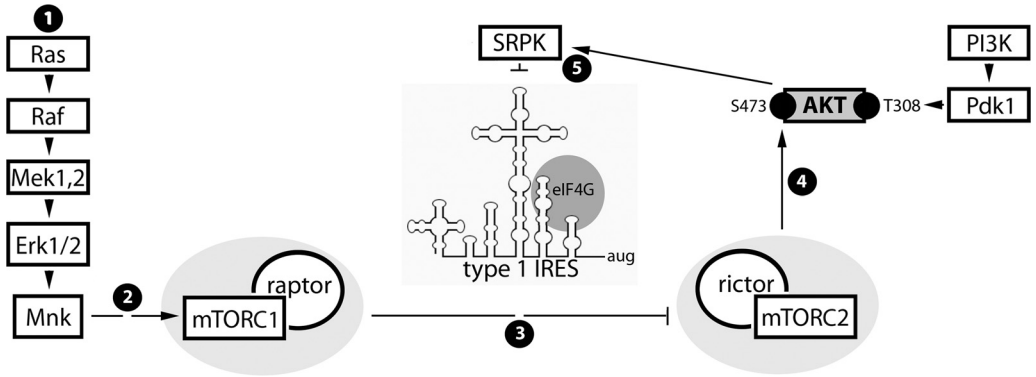

FIG 9 Proposed signal and functional relationships emerging from the present study and the companion report (13). (Step 1) Constitutive Raf-MEK-ERK1/2 signals in GBM cause MNK activation. (Step 2) MNK modulates mTORC1, possibly by intercepting inhibitory PRAS40-raptor binding (36). (Step 3) Our data suggest that MNK-mediated mTORC1 activation represses mTORC2. (Step 4) Inhibition of mTORC2 prevents phosphorylation of AKT(S473) and reduces mTORC2-AKT signaling to SRPK. (Step 5) SRPK-mediated regulation of viral cap-independent translation may occur via SR proteins, e.g., SRp20, a proposed PV ITAF (10). Phosphorylation of SR proteins by SRPK enhances their nuclear import (42) and decreases their affinity for RNA (43). Thus, MNK stimulation of viral m^7G cap-independent translation may be due to SRPK inhibition, favoring SR protein cytoplasmic retention and viral RNA binding.

a broad influence of MNK on posttranscriptional gene-regulatory systems far beyond its classic role as the eIF4E(S209) kinase.

We previously reported that PI3K inhibition enhances PVSRIPO oncolysis in a GBM xenograft model (23). This was anticipated, because PI3K downstream signals to mTORC1 inactivate the 4EBPs, which in their active state enhance IRES-mediated translation (32). However, given our finding that MNK represses SRPK (which is controlled by PI3K/AKT signaling; [17]) to stimulate PVSRIPO translation (13), we tested whether PI3K-mediated effects on type 1 IRES-mediated translation are due to its role in regulating SRPK. We determined that, while 4EBP inactivation (with rapa) subtly enhances the PVSRIPO translation rate, the IRES-suppressive effect of PI3K activation is attributable to SRPK. This implicates SRPK as a key determinant of picornaviral type 1 IRES competence.

The central finding in this study that MNK acts on SRPK by impeding AKT(S473) phosphorylation by mTORC2 (Fig. 9) supports earlier evidence that AKT has important roles in the regulation of SRPK partitioning and activity (17). Intuitively, AKT signal attenuation through MNK as a mechanism of PVSRIPO tumor-selective cytotoxicity seems implausible, given the frequency of PI3K upregulation in neoplasia. However, HeLa cells with very high intrinsic PI3K signaling respond to IGF1 with dissociation of nuclear speckles and strongly enhanced p-AKT(S473/T308). In U87 glioma cells, which have PTEN deleted, IGF1-mediated activation of AKT delayed PVSRIPO translation and cytotoxicity. MNK inhibition with CGP57380 produced AKT activation in HeLa and U87 cells, despite inherently high levels of PI3K-AKT signaling. Together, our observations suggest that downstream of overactive PI3K signaling (i.e., with PTEN deletion or activating *PIK3CG* mutations), both AKT and SRPK maintain a level of adaptive plasticity that is accomplished through MNK (and possibly other signal connections). The balance between PI3K-AKT and Raf-ERK1/2-MNK signaling necessary to prevent constitutive SRPK activation facilitates PVSRIPO oncolysis. The finding that MNK diminishes AKT(S473) phosphorylation (by mTORC2) adds to the rapidly accumulating evidence for extensive, multilayered Raf-ERK1/2 cross talk with PI3K-AKT (33). Thus, in the malignant context, MNK, along with other signaling nodes, maintains homeostasis that prevents excessive activation of AKT signaling, such as overactive SRPK in the present study. Such cross talk is likely necessary to achieve a balance between PI3K and Raf-ERK1/2 signaling commensurate with life, because chronic aberrant AKT activity is lethal in cancer cells (34).

Although the MNK-AKT-SRPK connection has been the primary focus of the present and accompanying studies (13) because SRPK controls PVSRIPO IRES competence/cytotoxicity in malignancy, our observation that MNK regulates mTORC1 inversely to mTORC2 is of the utmost biological significance. A relationship between MNK and mTOR signaling is in line with several recent findings, including that (i) MNK activity is correlated with enhanced p-4EBP1(S65), an mTORC1 substrate (35); (ii) MNK2 binds to raptor and prevents PRAS40 association with mTORC1, an endogenous inhibitor of mTORC1 activity (36); and (iii) rapa-induced survival feedback signals leading to MNK activation could represent a feedback loop for compensatory mTORC1 stimulation (37, 38). Our studies indicate that MNK inhibition with CGP57380 activates mTORC2 [and AKT(S473) phosphorylation] while diminishing phosphorylation of mTORC1 targets. Accordingly, expression of constitutively active MNK1 enhanced mTORC1 activity while reducing p-AKT(S473). Accumulating evidence for key roles of MNK in protumorigenic and prosurvival gene-regulatory functions (39) may well be explained by its role in regulating mTORC1.

At this point, it remains unclear how MNK acts on mTOR. It was proposed that MNK2 specifically associates with the mTORC1 complex, thus preventing inhibitory PRAS40-mTORC1 interactions (36). This may result in activation of mTORC1 and, consequently, mTORC2 suppression. This is seemingly contradicted by our finding that rapa did not prevent AKT(S473) phosphorylation (by mTORC2) upon MNK inhibition with CGP57380 (Fig. 6A). However, rapa affects only phosphorylation of select mTORC1 substrates (40, 41).

Our work described in this study and a companion report (13) revealed a network of surprisingly close integration of MNK and mTOR/AKT signals that impinge on SRPK and its role in posttranscriptional gene regulation (Fig. 9). This network controls picornaviral type 1 IRES competence and, by extension, PVSRIPO

cytotoxicity and tumor cell killing. Our data suggest that major signal-responsive elements in type 1 IRES-mediated translation may be RNA-binding proteins with ITAF roles, e.g., PCBP2/SR proteins, which are controlled by the AKT-SRPK axis.

ACKNOWLEDGMENTS

We thank R. Fukunaga (Osaka University, Osaka, Japan) for providing MNK1/2 dko MEFs.

This research was supported by PHS awards CA124756 (M.G.) and 5T32CA009111 (M.B.), by the National Center for Advancing Translational Sciences of the NIH (UL1TR001117), and by the Southeastern Brain Tumor Foundation.

REFERENCES

1. **Pelletier J, Sonenberg N.** 1988. Internal initiation of translation of eukaryotic mRNA directed by a sequence derived from poliovirus RNA. Nature **334:**320–325. http://dx.doi.org/10.1038/334320a0.
2. **Jang SK, Krausslich HG, Nicklin MJ, Duke GM, Palmenberg AC, Wimmer E.** 1988. A segment of the 5′ nontranslated region of encephalomyocarditis virus RNA directs internal entry of ribosomes during in vitro translation. J. Virol. **62:**2636–2643.
3. **Spahn CM, Kieft JS, Grassucci RA, Penczek PA, Zhou K, Doudna JA, Frank J.** 2001. Hepatitis C virus IRES RNA-induced changes in the conformation of the 40S ribosomal subunit. Science **291:**1959–1962. http://dx.doi.org/10.1126/science.1058409.
4. **Sweeney TR, Abaeva IS, Pestova TV, Hellen CU.** 2014. The mechanism of translation initiation on type 1 picornavirus IRESs. EMBO J. **33:**76–92. http://dx.doi.org/10.1002/embj.201386124.
5. **Yu Y, Abaeva IS, Marintchev A, Pestova TV, Hellen CU.** 2011. Common conformational changes induced in type 2 picornavirus IRESs by cognate trans-acting factors. Nucleic Acids Res. **39:**4851–4865. http://dx.doi.org/10.1093/nar/gkr045.
6. **Parsyan A, Svitkin Y, Shahbazian D, Gkogkas C, Lasko P, Merrick WC, Sonenberg N.** 2011. mRNA helicases: the tacticians of translational control. Nat. Rev. Mol. Cell Biol. **12:**235–245. http://dx.doi.org/10.1038/nrm3083.
7. **Marcotrigiano J, Lomakin IB, Sonenberg N, Pestova TV, Hellen CU, Burley SK.** 2001. A conserved HEAT domain within eIF4G directs assembly of the translation initiation machinery. Mol. Cell **7:**193–203. http://dx.doi.org/10.1016/S1097-2765(01)00167-8.
8. **Pestova TV, Shatsky IN, Hellen CU.** 1996. Functional dissection of eukaryotic initiation factor 4F: the 4A subunit and the central domain of the 4G subunit are sufficient to mediate internal entry of 43S preinitiation complexes. Mol. Cell. Biol. **16:**6870–6878.
9. **Blyn LB, Swiderek KM, Richards O, Stahl DC, Semler BL, Ehrenfeld E.** 1996. Poly(rC) binding protein 2 binds to stem-loop IV of the poliovirus RNA 5′ noncoding region: identification by automated liquid chromatography-tandem mass spectrometry. Proc. Natl. Acad. Sci. U. S. A. **93:**11115–11120. http://dx.doi.org/10.1073/pnas.93.20.11115.
10. **Bedard KM, Daijogo S, Semler BL.** 2007. A nucleo-cytoplasmic SR protein functions in viral IRES-mediated translation initiation. EMBO J. **26:**459–467. http://dx.doi.org/10.1038/sj.emboj.7601494.
11. **Merrill MK, Dobrikova EY, Gromeier M.** 2006. Cell-type-specific repression of internal ribosome entry site activity by double-stranded RNA-binding protein 76. J. Virol. **80:**3147–3156. http://dx.doi.org/10.1128/JVI.80.7.3147-3156.2006.
12. **Gromeier M, Lachmann S, Rosenfeld MR, Gutin PH, Wimmer E.** 2000. Intergeneric poliovirus recombinants for the treatment of malignant glioma. Proc. Natl. Acad. Sci. U. S. A. **97:**6803–6808. http://dx.doi.org/10.1073/pnas.97.12.6803.
13. **Brown MC, Bryant JD, Dobrikova EY, Shveygert M, Bradrick SS, Chandramohan V, Bigner DD, Gromeier M.** 2014. Induction of viral, 7-methyl-guanosine cap-independent translation and oncolysis by mitogen-activated protein kinase-interacting kinase-mediated effects on the serine/arginine-rich protein kinase. J. Virol. **88:**13135–13148. http://dx.doi.org/10.1128/JVI.01883-14.
14. **Pyronnet S, Imataka H, Gingras AC, Fukunaga R, Hunter T, Sonenberg N.** 1999. Human eukaryotic translation initiation factor 4G (eIF4G) recruits mnk1 to phosphorylate eIF4E. EMBO J. **18:**270–279. http://dx.doi.org/10.1093/emboj/18.1.270.
15. **Shveygert M, Kaiser C, Bradrick SS, Gromeier M.** 2010. Regulation of eukaryotic initiation factor 4E (eIF4E) phosphorylation by mitogen-activated protein kinase occurs through modulation of Mnk1-eIF4G interaction. Mol. Cell. Biol. **30:**5160–5167. http://dx.doi.org/10.1128/MCB.00448-10.
16. **Waskiewicz AJ, Flynn A, Proud CG, Cooper JA.** 1997. Mitogen-activated protein kinases activate the serine/threonine kinases Mnk1 and Mnk2. EMBO J. **16:**1909–1920. http://dx.doi.org/10.1093/emboj/16.8.1909.
17. **Zhou Z, Qiu J, Liu W, Zhou Y, Plocinik RM, Li H, Hu Q, Ghosh G, Adams JA, Rosenfeld MG, Fu XD.** 2012. The Akt-SRPK-SR axis constitutes a major pathway in transducing EGF signaling to regulate alternative splicing in the nucleus. Mol. Cell **47:**422–433. http://dx.doi.org/10.1016/j.molcel.2012.05.014.
18. **Ueda T, Watanabe-Fukunaga R, Fukuyama H, Nagata S, Fukunaga R.** 2004. Mnk2 and Mnk1 are essential for constitutive and inducible phosphorylation of eukaryotic initiation factor 4E but not for cell growth or development. Mol. Cell. Biol. **24:**6539–6549. http://dx.doi.org/10.1128/MCB.24.15.6539-6549.2004.
19. **Kaiser C, Dobrikova EY, Bradrick SS, Shveygert M, Herbert JT, Gromeier M.** 2008. Activation of cap-independent translation by variant eukaryotic initiation factor 4G in vivo. RNA **14:**2170–2182. http://dx.doi.org/10.1261/rna.1171808.
20. **Dobrikova EY, Goetz C, Walters RW, Lawson SK, Peggins JO, Muszynski K, Ruppel S, Poole K, Giardina SL, Vela EM, Estep JE, Gromeier M.** 2012. Attenuation of neurovirulence, biodistribution, and shedding of a poliovirus: rhinovirus chimera after intrathalamic inoculation in Macaca fascicularis. J. Virol. **86:**2750–2759. http://dx.doi.org/10.1128/JVI.06427-11.
21. **Bradrick SS, Dobrikova EY, Kaiser C, Shveygert M, Gromeier M.** 2007. Poly(A)-binding protein is differentially required for translation mediated by viral internal ribosome entry sites. RNA **13:**1582–1593. http://dx.doi.org/10.1261/rna.556107.
22. **Dobrikov M, Dobrikova E, Shveygert M, Gromeier M.** 2011. Phosphorylation of eukaryotic translation initiation factor 4G1 (eIF4G1) by protein kinase C{alpha} regulates eIF4G1 binding to Mnk1. Mol. Cell. Biol. **31:**2947–2959. http://dx.doi.org/10.1128/MCB.05589-11.
23. **Goetz C, Everson RG, Zhang LC, Gromeier M.** 2010. MAPK signal-integrating kinase controls cap-independent translation and cell type-specific cytotoxicity of an oncolytic poliovirus. Mol. Ther. **18:**1937–1946. http://dx.doi.org/10.1038/mt.2010.145.
24. **Sarbassov DD, Guertin DA, Ali SM, Sabatini DM.** 2005. Phosphorylation and regulation of Akt/PKB by the rictor-mTOR complex. Science **307:**1098–1101. http://dx.doi.org/10.1126/science.1106148.
25. **Oh WJ, Wu CC, Kim SJ, Facchinetti V, Julien LA, Finlan M, Roux PP, Su B, Jacinto E.** 2010. mTORC2 can associate with ribosomes to promote cotranslational phosphorylation and stability of nascent Akt polypeptide. EMBO J. **29:**3939–3951. http://dx.doi.org/10.1038/emboj.2010.271.
26. **McDonald PC, Oloumi A, Mills J, Dobreva I, Maidan M, Gray V, Wederell ED, Bally MB, Foster LJ, Dedhar S.** 2008. Rictor and integrin-linked kinase interact and regulate Akt phosphorylation and cancer cell survival. Cancer Res. **68:**1618–1624. http://dx.doi.org/10.1158/0008-5472.CAN-07-5869.
27. **Dibble CC, Asara JM, Manning BD.** 2009. Characterization of Rictor phosphorylation sites reveals direct regulation of mTOR complex 2 by S6K1. Mol. Cell. Biol. **29:**5657–5670. http://dx.doi.org/10.1128/MCB.00735-09.
28. **Sarbassov DD, Ali SM, Sengupta S, Sheen JH, Hsu PP, Bagley AF, Markhard AL, Sabatini DM.** 2006. Prolonged rapamycin treatment inhibits mTORC2 assembly and Akt/PKB. Mol. Cell **22:**159–168. http://dx.doi.org/10.1016/j.molcel.2006.03.029.
29. **Furic L, Rong L, Larsson O, Koumakpayi IH, Yoshida K, Brueschke A, Petroulakis E, Robichaud N, Pollak M, Gaboury LA, Pandolfi PP, Saad F, Sonenberg N.** 2010. eIF4E phosphorylation promotes tumorigenesis and is associated with prostate cancer progression. Proc. Natl. Acad. Sci. U. S. A. **107:**14134–14139. http://dx.doi.org/10.1073/pnas.1005320107.
30. **Ueda T, Sasaki M, Elia AJ, Chio II, Hamada K, Fukunaga R, Mak TW.** 2010. Combined deficiency for MAP kinase-interacting kinase 1 and 2 (Mnk1 and Mnk2) delays tumor development. Proc. Natl. Acad. Sci. U. S. A. **107:**13984–13990. http://dx.doi.org/10.1073/pnas.1008136107.
31. **Wendel HG, Silva RL, Malina A, Mills JR, Zhu H, Ueda T, Watanabe-Fukunaga R, Fukunaga R, Teruya-Feldstein J, Pelletier J, Lowe SW.** 2007. Dissecting eIF4E action in tumorigenesis. Genes Dev. **21:**3232–3237. http://dx.doi.org/10.1101/gad.1604407.
32. **Svitkin YV, Herdy B, Costa-Mattioli M, Gingras AC, Raught B, Sonen-**

berg N. 2005. Eukaryotic translation initiation factor 4E availability controls the switch between cap-dependent and internal ribosomal entry site-mediated translation. Mol. Cell. Biol. **25:**10556–10565. http://dx.doi.org/10.1128/MCB.25.23.10556-10565.2005.

33. **Mendoza MC, Er EE, Blenis J.** 2011. The Ras-ERK and PI3K-mTOR pathways: cross-talk and compensation. Trends Biochem. Sci. **36:**320–328. http://dx.doi.org/10.1016/j.tibs.2011.03.006.
34. **van Gorp AG, Pomeranz KM, Birkenkamp KU, Hui RC, Lam EW, Coffer PJ.** 2006. Chronic protein kinase B (PKB/c-akt) activation leads to apoptosis induced by oxidative stress-mediated Foxo3a transcriptional up-regulation. Cancer Res. **66:**10760–10769. http://dx.doi.org/10.1158/0008-5472.CAN-06-1111.
35. **Grzmil M, Huber RM, Hess D, Frank S, Hynx D, Moncayo G, Klein D, Merlo A, Hemmings BA.** 2014. MNK1 pathway activity maintains protein synthesis in rapalog-treated gliomas. J. Clin. Invest. **124:**742–754. http://dx.doi.org/10.1172/JCI70198.
36. **Hu SI, Katz M, Chin S, Qi X, Cruz J, Ibebunjo C, Zhao S, Chen A, Glass DJ.** 2012. MNK2 inhibits eIF4G activation through a pathway involving serine-arginine-rich protein kinase in skeletal muscle. Sci. Signal **5:**ra14. http://dx.doi.org/10.1126/scisignal.2002466.
37. **Sun SY, Rosenberg LM, Wang X, Zhou Z, Yue P, Fu H, Khuri FR.** 2005. Activation of Akt and eIF4E survival pathways by rapamycin-mediated mammalian target of rapamycin inhibition. Cancer Res. **65:**7052–7058. http://dx.doi.org/10.1158/0008-5472.CAN-05-0917.
38. **Wang X, Yue P, Chan CB, Ye K, Ueda T, Watanabe-Fukunaga R, Fukunaga R, Fu H, Khuri FR, Sun SY.** 2007. Inhibition of mammalian target of rapamycin induces phosphatidylinositol 3-kinase-dependent and Mnk-mediated eukaryotic translation initiation factor 4E phosphorylation. Mol. Cell. Biol. **27:**7405–7413. http://dx.doi.org/10.1128/MCB.00760-07.
39. **Diab S, Kumarasiri M, Yu M, Teo T, Proud C, Milne R, Wang S.** 2014. MAP kinase-interacting kinases—emerging targets against cancer. Chem. Biol. **21:**441–452. http://dx.doi.org/10.1016/j.chembiol.2014.01.011.
40. **Kang SA, Pacold ME, Cervantes CL, Lim D, Lou HJ, Ottina K, Gray NS, Turk BE, Yaffe MB, Sabatini DM.** 2013. mTORC1 phosphorylation sites encode their sensitivity to starvation and rapamycin. Science **341:**1236566. http://dx.doi.org/10.1126/science.1236566.
41. **Thoreen CC, Kang SA, Chang JW, Liu Q, Zhang J, Gao Y, Reichling LJ, Sim T, Sabatini DM, Gray NS.** 2009. An ATP-competitive mammalian target of rapamycin inhibitor reveals rapamycin-resistant functions of mTORC1. J. Biol. Chem. **284:**8023–8032. http://dx.doi.org/10.1074/jbc.M900301200.
42. **Lai MC, Lin RI, Tarn WY.** 2001. Transportin-SR2 mediates nuclear import of phosphorylated SR proteins. Proc. Natl. Acad. Sci. U. S. A. **98:**10154–10159. http://dx.doi.org/10.1073/pnas.181354098.
43. **Sanford JR, Gray NK, Beckmann K, Caceres JF.** 2004. A novel role for shuttling SR proteins in mRNA translation. Genes Dev. **18:**755–768. http://dx.doi.org/10.1101/gad.286404.